Time-dependent physics of double-tunnel junctions

Vincent Talbo*, Javier Mateos*, Sylvie Retailleau†, Philippe Dollfus† and Tomás González*
*Departamento de Física Aplicada, Universidad de Salamanca, Plaza de la Merced S/N, E-37008 Salamanca, Spain
†Institut d'Electronique Fondamentale, Université Paris-Sud, CNRS UMR 8622, F-91405 Orsay, France
e-mail: vtalbo@usal.es

***Abstract*—In this work, we investigate and explain the time-dependent behavior of shot noise in Silicon quantum dot-based double-tunnel junctions by means of a three-dimensional self-consistent simulation and a Monte-Carlo algorithm following the time evolution of the system. We demonstrate the strong link between autocorrelation functions and electron waiting time distributions, i.e, the time between two consecutive tunnel events through a given junction. Moreover, we separate and analyze the contribution of each different path - evolution of the number of electrons in the quantum dot between two consecutive tunnel events through the same junction - to understand clearly the behavior of auto-correlations and waiting time distributions in the case of a 3-state system.**

I. Introduction

The recent progresses in the fabrication of Silicon quantum dot (QD)-based single-electron devices (SEDs) allowed the observation of well-defined Coulomb oscillations at room-temperature in single-electron transistors (SETs), paving the way of future applications [1]–[5].

Moreover, detection of single-electron events are now performed experimentally, giving access to current fluctuations [6], and in particular measurements of shot noise (SN), which gives more information on electronic transport than conductance and thus has been intensively studied over the last decades [7]. Most of the theoretical models for SN in SEDs are based on the full counting statistics tool (FCS) [8], [9], calculating all zero-frequency current-correlations from probability distributions of number of electrons transferred during a long period of time. The spectral density $S(\omega)$ associated to SN is characterized at zero-frequency by its deviation to fully Poissonian SN $2eI$, where I is the mean current, and the Fano factor is defined as the ratio $F = S(0)/2eI$ (If $F < 1 (> 1)$ then the electronic transport is sub-(super-)Poissonian). However, the frequency- and time-dependent physics of SN is less explored. On this purpose, a new method emerged recently, focusing on the distribution of time delays between two consecutive tunnel events in a barrier, also called waiting time distributions (WTDs) [10], [11].

To simulate accurately the electronic structure of a Si QD in an SED, and then their electronic characteristics, we use the homemade 3D self-consistent code SENS (Single-Electron Nanodevices Simulation), initially developed for Si QD-based double-tunnel junctions (DTJs) [12], then extended to double-dot structures by introducing phonon contribution [13] and SETs by including the effect of a gate [14]. In this work, we simulate a DTJ, schematized in Fig. 1, with the SENS code, and calculate the autocorrelation functions (AFs) and WTDs from the results of a Monte-Carlo algorithm. The strong correlation between AFs and WTDs is enlightened for different biases, corresponding to different transport regime. Finally, we separate and analyze the different contribution of each basic path, i.e. the evolution of the number of electrons in the dot between two consecutive tunnel events through the source junction, in the case of a 3-state QD (0, 1 or 2 electrons in the QD) to provide a clear and intuitive understanding of the time-dependent physics of SN in DTJs.

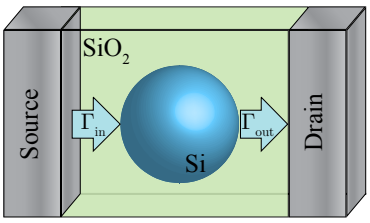

Fig. 1. Schematic view of a DTJ.

II. SENS code

The first stage of the simulation relies on the calculation of the electronic structure of the QD according to the bias voltage and the number of electrons inside it by solving the Poisson-Schrödinger coupled equations within the Hartree and effective mass approximations, proven to be correct for Si-QDs of radius greater than 1.5 nm [15], [16]. Thanks to the Hartree method, the wavefunctions depend on the number of electron N in the QD.

The resulting wavefunctions are then used to compute the tunnel transfer rates source-to-dot $\Gamma_{\rm in}(N)$ and dot-to-drain $\Gamma_{\rm out}(N)$ by means of the Fermi golden rule and Bardeen formalism. Finally, the transfer rates are introduced in a Monte-Carlo algorithm to follow the time-evolution of the number of electrons in the dot, giving access to all electrical characteristics, such as current, WTDs and AFs. Analytic expressions have been derived for AFs and WTDs for the case of a maximum of 2 electrons in the QD, which reproduce exactly the predictions from MC simulations.

III. Results and discussion

The simulated DTJ consists in a 8-nm-diameter Si-QD, with source and drain tunnel barriers of 1.2 nm and 1.8 nm thicknesses, respectively. The current and Fano factor, F, are shown in Fig. 2. The current shows a positive differential conductance in the first two Coulomb stairs, while a negative differential conductance is observed in subsequent stairs. F decreases on the two first stairs, reaching its minimum just before the third step, and then increases until reaching its maximum value at the beginning of the fourth step. The

978-1-4799-8108-3/151$31.00 ©2015 IEEE

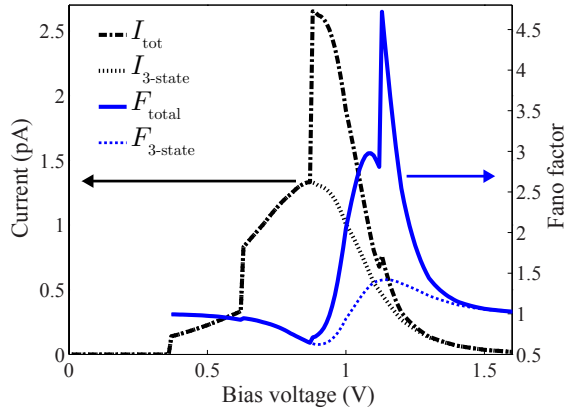

Fig. 2. Current and Fano factor in the normal case and the 3-state case as a function of the applied voltage.

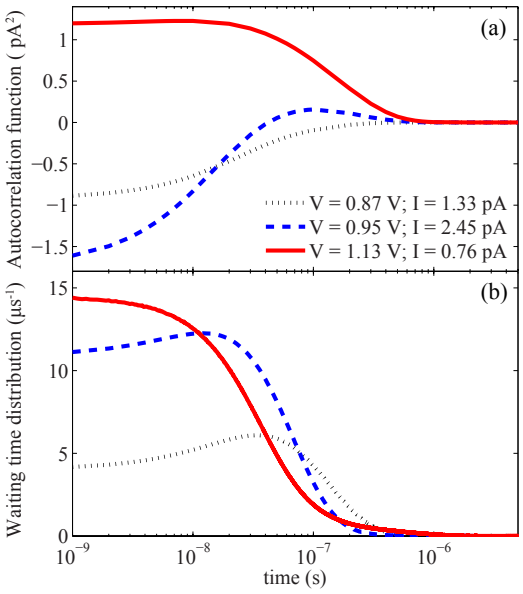

Fig. 3. (a) AFs and (b) WTDs as a function of the delay time for 3 different biases corresponding to the minimum ($V = 0.87$ V), maximum ($V = 1.13$ V) and Poissonian ($V = 0.95$ V) values of the Fano factor.

behaviour of the current and F are explained in previous articles [12], [17].

AFs and WTDs for three particular biases (minimum, maximum and Poissonian Fano factor) are given in Fig. 3. In the case $V = 1.13$ V, where F is maximum, the maximum of WTD occurs at the shortest times. The current pulses are thus positively correlated for low times and the AF shows positive values that vanish for times around 10^{-6} s, when the correlations are lost. Conversely, the WTDs show a maximum at intermediate times for the two other cases. This means that it is more unlikely to find another current pulse before this time-delay, and thus the AFs shows negative values at lower times. For delay times approaching the maximum of the WTD the probability of having current pulses with such delay times is increased, thus providing positive values of the AF. We have to remark that at long times the time dependence of AF

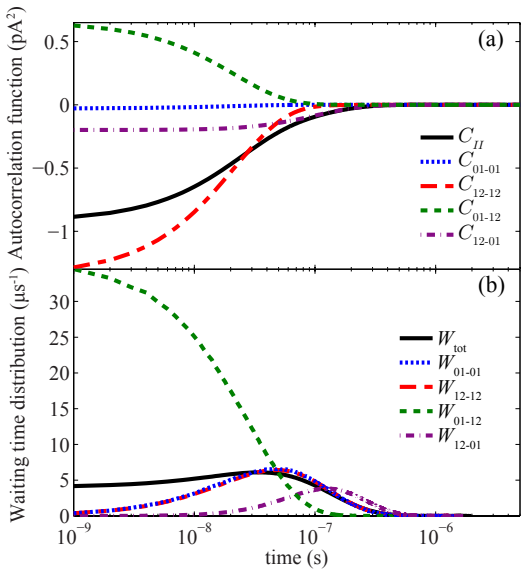

Fig. 4. (a) Auto- and cross-correlation functions and (b) WTDs between (01) and (12) current pulses as a function of time, for a bias $V = 0.87$ V corresponding to the minimum of the Fano factor F.

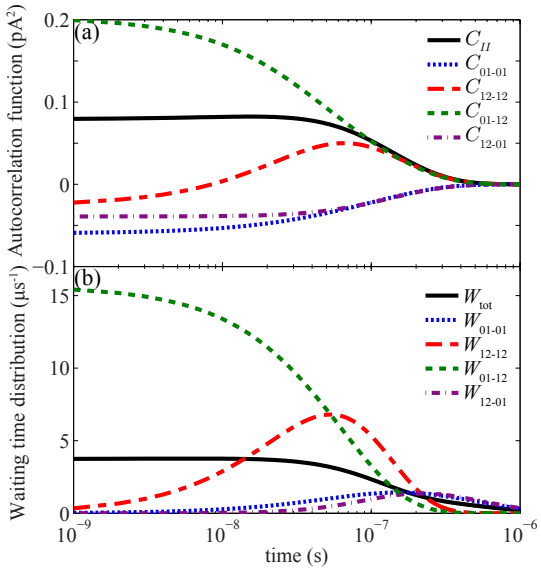

Fig. 5. (a) Auto- and cross-correlation functions and (b) WTDs between (01) and (12) current pulses as a function of time, for a bias $V = 1.15$ V corresponding to the maximum of the Fano factor F.

and WTD are slightly different, as the WTDs concern only two consecutive current pulses, while the AFs correlate any tunnel event with another, not only consecutive ones. As a consequence AFs tend to vanish for longer times than WTDs.

To go deeper in the understanding of the origin of shot noise suppression/enhancement, we separate the contributions of the different types of current pulses to the AFs. For simplicity, we limit ourselves to a 3-state case, meaning that the QD can only contain a maximum of 2 electrons. The

TABLE I. PROBABILITIES OF BASIC PATHS FOR THE EXTREME VALUES OF THE FANO FACTOR IN THE 3-STATE CASE.

basic paths	$V = 0.9$ V $F = 0.62$	$V = 1.15$ V $F = 1.42$
01-01	2 %	36 %
12-12	70 %	16 %
01-12	14 %	24 %
12-01	14 %	24 %

resulting current and Fano factor are shown in Fig. 2. The only possible evolution of the number of electrons in the dot which can provide current pulses through source tunnel oxide are then $0 \rightarrow 1$ (01) and $1 \rightarrow 2$ (12). The probabilities of having two consecutive (01) and (12) pulses, (01) followed by (12) pulses, and inversely, are given in TABLE I for two different biases, corresponding to the maximum and the minimum of Fano factor in the 3-state case. We have then plotted in Fig. 4(a) and Fig. 5(a) the auto- and cross-correlations of current pulses originated from (01) and (12) transitions for those biases. The corresponding WTDs are shown in Fig. 4(b) and Fig. 5(b).

As no other intermediate transition is necessary to have consecutive (01)-(12) events, their contributions C_{01-12} are always positive, and their maximum is reached at zero time, where the WTD W_{01-12} is maximum. On the other hand, WTDs are minimum at low times for the other 3 types of consecutive events, since intermediate transitions are needed between two consecutive (01) or (12) pulses, implying a negative contribution of C_{01-01}, C_{12-12} and C_{12-01} to the AFs. AFs increase with their respective WTDs, until reaching their maximum value. They can then generate positive correlations, for the times where two current pulses are the most probable, in parallel to the maximum of the WTDs. Moreover, the weight of each of the contributions of the four different correlations is given by the amount of events of each type, given in TABLE I.

In Fig. 4, corresponding to the minimum of the Fano factor, the major contribution of current comes from (12) transitions (87 % of the total current). Then, the total AF C_{II} essentially follows the behaviour of C_{12-12}, i.e. the AF of (12) pulses. C_{12-12} is negative for low times and then increases with its corresponding WTD W_{12-12} until reaching its maximum and the uncorrelated value for long times. However, C_{12-12} is only slightly positive around its maximum, and thus does not compensate the negative contribution of C_{01-01} and C_{12-01} on the total AF C_{II}, which thus remains negative.

Inversely, in the case of the maximum of Fano factor shown in Fig. 5, no pulse is really more probable than another. The negative contribution of (12) pulses C_{12-12} on the total AF is then weaker than in the previous case. Hence, the positive contribution of C_{01-12} is not compensated by the 3 other transitions, and the total AF C_{II} is always positive, which results in a super-Poissonian behaviour.

IV. CONCLUSION

Thanks to the ability of SENS code to simulate accurately the electronic behaviour of a Si QD-based DTJ, we have calculated the current auto-correlations and waiting time distributions in both sub and super-Poissonian regimes, and showed their close relation. Thanks to the Hartree method, giving access to tunnel transfer rates depending on the number of electrons in the dot, we could separate AFs and WTDs in different contributions depending on the type of transition involved in a current pulse; and linked to their probabilities, we have been able to offer a clear understanding of current auto-correlation functions, thus the time-dependent physics governing the device.

ACKNOWLEDGMENT

This work has been partially supported by the Dirección General de Investigación Científica y Técnica (MINECO) through Project TEC2013-41640-R and by the Junta de Castilla y León through Project SA052U13. V. Talbo wants to thank the European Social Fund (ESF) for financing his postdoctoral contract.

REFERENCES

[1] V. Deshpande, S. Barraud, X. Jehl, R. Wacquez, M. Vinet, R. Coquand, B. Roche, B. Voisin, F. Triozon, C. Vizioz *et al.*, "Scaling of trigate nanowire (nw) mosfets to sub-7nm width: 300k transition to single electron transistor," *Solid-State Electronics*, vol. 84, pp. 179–184, 2013. [Online]. Available: http://www.sciencedirect.com/science/article/pii/S0038110113000762

[2] S. Lee, Y. Lee, E. B. Song, and T. Hiramoto, "Observation of single electron transport via multiple quantum states of a silicon quantum dot at room temperature," *Nano Letters*, vol. 14, no. 1, pp. 71–77, 2014.

[3] S. J. Shin, C. S. Jung, B. J. Park, T. K. Yoon, J. J. Lee, S. J. Kim, J. B. Choi, Y. Takahashi, and D. G. Hasko, "Si-based ultrasmall multiswitching single-electron transistor operating at room-temperature," *Applied Physics Letters*, vol. 97, no. 10, p. 103101, 2010. [Online]. Available: http://link.aip.org/link/?APL/97/103101/1

[4] S. J. Shin, J. J. Lee, H. J. Kang, J. B. Choi, S.-R. E. Yang, Y. Takahashi, and D. G. Hasko, "Room-temperature charge stability modulated by quantum effects in a nanoscale silicon island," *Nano Letters*, vol. 11, no. 4, pp. 1591–1597, 2011. [Online]. Available: http://dx.doi.org/10.1021/nl1044692

[5] Y. Tanahashi, R. Suzuki, T. Saraya, and T. Hiramoto, "Peak position control of coulomb blockade oscillations in silicon single-electron transistors with floating gate operating at room temperature," *Japanese Journal of Applied Physics*, vol. 53, no. 4S, p. 04EJ08, 2014. [Online]. Available: http://stacks.iop.org/1347-4065/53/i=4S/a=04EJ08

[6] N. Ubbelohde, C. Fricke, C. Flindt, F. Hohls, and R. J. Haug, "Measurement of finite-frequency current statistics in a single-electron transistor," *Nature Communications*, vol. 3, pp. 612–, Jan. 2012. [Online]. Available: http://dx.doi.org/10.1038/ncomms1620

[7] Y. Blanter and M. Büttiker, "Shot noise in mesoscopic conductors," *Physics Reports*, vol. 336, no. 1–2, pp. 1 – 166, 2000. [Online]. Available: http://www.sciencedirect.com/science/article/pii/S0370157399001234

[8] L. S. Levitov, H. Lee, and G. B. Lesovik, "Electron counting statistics and coherent states of electric current," *Journal of Mathematical Physics*, vol. 37, no. 10, pp. 4845–4866, 1996. [Online]. Available: http://scitation.aip.org/content/aip/journal/jmp/37/10/10.1063/1.531672

[9] D. A. Bagrets and Y. V. Nazarov, "Full counting statistics of charge transfer in coulomb blockade systems," *Phys. Rev. B*, vol. 67, p. 085316, Feb 2003. [Online]. Available: http://link.aps.org/doi/10.1103/PhysRevB.67.085316

[10] T. Brandes, "Waiting times and noise in single particle transport," *Annalen der Physik*, vol. 17, no. 7, pp. 477–496, 2008. [Online]. Available: http://dx.doi.org/10.1002/andp.200810306

[11] M. Albert, G. Haack, C. Flindt, and M. Büttiker, "Electron waiting times in mesoscopic conductors," *Phys. Rev. Lett.*, vol. 108, p. 186806, May 2012. [Online]. Available: http://link.aps.org/doi/10.1103/PhysRevLett.108.186806

[12] J. Sée, P. Dollfus, and S. Galdin, "Theoretical investigation of negative differential conductance regime of silicon nanocrystal single-electron devices," *Electron Devices, IEEE Transactions on*, vol. 53, no. 5, pp. 1268–1273, May 2006.

[13] A. Valentin, S. Galdin-Retailleau, and P. Dollfus, "Phonon effect on single-electron transport in two-dot semiconductor devices," *Journal of Applied Physics*, vol. 106, no. 4, p. 044501, 2009. [Online]. Available: http://link.aip.org/link/?JAP/106/044501/1

[14] V. Talbo, S. Galdin-Retailleau, A. Valentin, and P. Dollfus, "Physical simulation of silicon-nanocrystal-based single-electron transistors," *Electron Devices, IEEE Transactions on*, vol. 58, no. 10, pp. 3286–3293, Oct 2011.

[15] J. Sée, P. Dollfus, and S. Galdin, "Comparison between a sp^3d^5 tight-binding and an effective-mass description of silicon quantum dots," *Phys. Rev. B*, vol. 66, p. 193307, Nov 2002. [Online]. Available: http://link.aps.org/doi/10.1103/PhysRevB.66.193307

[16] J. Sée, P. Dollfus, and S. Galdin, "Comparison of a density functional theory and a hartree treatment of silicon quantum dot," *Journal of Applied Physics*, vol. 92, no. 6, pp. 3141–3146, 2002. [Online]. Available: http://scitation.aip.org/content/aip/journal/jap/92/6/10.1063/1.1499524

[17] V. Talbo, D. Querlioz, S. Retailleau, and P. Dollfus, "Sub-and super-poissonian noise in si quantum dots using fully self-consistent 3d simulation," *Fluctuation and Noise Letters*, vol. 11, no. 03, p. 1242006, 2012. [Online]. Available: http://www.worldscientific.com/doi/abs/10.1142/S0219477512420060